Ultrahigh-Q one-dimensional photonic crystal nanocavities with modulated mode-gap barriers on SiO_2 claddings and on air claddings

Eiichi Kuramochi[1,2*], Hideaki Taniyama[1,2], Takasumi Tanabe[1,2], Kohei Kawasaki[1], Young-Geun Roh[1,2], and Masaya Notomi[1,2]

[1]*NTT Basic Research Laboratories, NTT Corporation, 3-1 Morinosato Wakamiya, Atsugi-shi, Kanagawa 243-0198, Japan*

[2]*CREST, Japan Agency of Science and Technology, 4-1-8 Honmachi, Kawaguchi, Saitama 332-0012, Japan*

**kuramoti@nttbrl.jp*

Abstract: We report designs for a silicon-on-insulator (SOI) one-dimensional (1D) photonic crystal (PhC) nanocavity with modulated mode-gap barriers based on the lowest dielectric band. These cavities have an ultrahigh theoretical quality factor (Q) of 10^7-10^8 while maintaining a very small modal volume of 0.6-2.0 $(\lambda/n)^3$, which are the highest Q for any nanocavities with SiO_2 under-cladding. We have fabricated these SOI 1D-PhC cavities and confirmed that they exhibited a Q of 3.6×10^5, which is also the highest measured Q for SOI-type PhC nanocavities. We have also applied the same design to 1D PhC cavities with air claddings, and found that they exhibit a theoretical quality factor higher than 10^9. The fabricated air-cladding 1D Si PhC cavities have showed a quality factor of 7.2×10^5, which is close to the highest Q value for 1D PhC cavities.

OCIS codes: (230.5298) Photonic crystals; (230.5750) Resonators.

References and links

1. P. R. Villeneuve, J. S. Foresi, J. Ferrera, E. R. Thoen, G. Steinmeyer, S. Fan, J. D. Joannopoulos, L. C. Kimerling, H. I. Smith, and E. P. Ippen, "Photonic-bandgap microcavities in optical waveguides," Nature **390**(6656), 143–145 (1997).
2. D. Peyrade, E. Silberstein, P. Lalanne, A. Talneau, and Y. Chen, "Short Bragg mirrors with adiabatic modal conversion," Appl. Phys. Lett. **81**(5), 829–831 (2002).
3. P. Velha, E. Picard, T. Charvolin, E. Hadji, J. C. Rodier, P. Lalanne, and D. Peyrade, "Ultra-High *Q*/*V* Fabry-Perot microcavity on SOI substrate," Opt. Express **15**(24), 16090–16096 (2007), http://www.opticsinfobase.org/abstract.cfm?URI=oe-15-24-16090.
4. A. R. Zain, N. P. Johnson, M. Sorel, and R. M. De La Rue, "Ultra high quality factor one dimensional photonic crystal/photonic wire micro-cavities in silicon-on-insulator (SOI)," Opt. Express **16**(16), 12084–12089 (2008), http://www.opticsinfobase.org/oe/abstract.cfm?URI=oe-16-16-12084.
5. M. Notomi, A. Shinya, S. Mitsugi, E. Kuramochi, and H.-Y. Ryu, "Waveguides, resonators and their coupled elements in photonic crystal slabs," Opt. Express **12**(8), 1551–1561 (2004), http://www.opticsinfobase.org/oe/abstract.cfm?URI=oe-12-8-1551.
6. Y. Akahane, T. Asano, B. S. Song, and S. Noda, "Fine-tuned high-*Q* photonic-crystal nanocavity," Opt. Express **13**(4), 1202–1214 (2005), http://www.opticsinfobase.org/abstract.cfm?URI=oe-13-4-1202.
7. B. S. Song, S. Noda, T. Asano, and Y. Akahane, "Ultra-high-*Q* photonic double-heterostructure nanocavity," Nat. Mater. **4**(3), 207–210 (2005).
8. E. Kuramochi, M. Notomi, M. Mitsugi, A. Shinya, T. Tanabe, and T. Watanabe, "Ultrahigh-*Q* photonic crystal nanocavities realized by the local width modulation of a line defect," Appl. Phys. Lett. **88**(4), 041112 (2006).
9. M. Notomi, E. Kuramochi, and H. Taniyama, "Ultrahigh-*Q* nanocavity with 1D photonic gap," Opt. Express **16**(15), 11095–11102 (2008), http://www.opticsinfobase.org/oe/abstract.cfm?URI=oe-16-15-11095.
10. P. B. Deotare, M. W. McCutcheon, I. W. Frank, M. Khan, and M. Lončar, "High quality factor photonic crystal nanobeam cavities," Appl. Phys. Lett. **94**(12), 121106 (2009).
11. M. Eichenfield, R. Camacho, J. Chan, K. J. Vahala, and O. Painter, "A picogram- and nanometre-scale photonic-crystal optomechanical cavity," Nature **459**(7246), 550–555 (2009).
12. L.-D. Haret, T. Tanabe, E. Kuramochi, and M. Notomi, "Extremely low power optical bistability in silicon demonstrated using 1D photonic crystal nanocavity," Opt. Express **17**(23), 21108–21117 (2009), http://www.opticsinfobase.org/oe/abstract.cfm?URI=oe-17-23-21108.

#128504 - $15.00 USD Received 18 May 2010; revised 25 Jun 2010; accepted 28 Jun 2010; published 12 Jul 2010

13. P. B. Deotare, M. W. McCutcheon, I. W. Frank, M. Khan, and M. Lončar, "Coupled photonic crystal nanobeam cavities," Appl. Phys. Lett. **95**(3), 031102 (2009).
14. M. Eichenfield, J. Chan, R. M. Camacho, K. J. Vahala, and O. Painter, "Optomechanical crystals," Nature **462**(7269), 78–82 (2009).
15. C. A. Barrious, "Ultrasensitive nanomechanical photonic sensor based on horizontal slot-waveguide resonator," IEEE Photon. Technol. Lett. **18**(22), 2419–2421 (2006).
16. C. Lee, and J. Thillaigovindan, "Optical nanomechanical sensor using a silicon photonic crystal cantilever embedded with a nanocavity resonator," Appl. Opt. **48**(10), 1797–1803 (2009), http://www.opticsinfobase.org/abstract.cfm?URI=ao-48-10-1797.
17. S. Kita, K. Nozaki, and T. Baba, "Refractive index sensing utilizing a cw photonic crystal nanolaser and its array configuration," Opt. Express **16**(11), 8174–8180 (2008), http://www.opticsinfobase.org/oe/abstract.cfm?URI=oe-16-11-8174.
18. T.-W. Lu, Y.-H. Hsiao, W.-D. Ho, and P.-T. Lee, "Photonic crystal heteroslab-edge microcavity with high quality factor surface mode for index sensing," Appl. Phys. Lett. **94**(14), 141110 (2009).
19. Y. A. Vlasov, N. Moll, S. J. McNab, T.-W. Lu, Y.-H. Hsiao, W.-D. Ho, and P.-T. Lee, "Mode mixing in asymmetric double-trench photonic crystal waveguides," J. Appl. Phys. **95**(9), 4538–4544 (2004).
20. Y. Tanaka, T. Asano, R. Hatsuta, and S. Noda, "Investigation of point-defect cavity formed in two-dimensional photonic crystal slab with one-sided dielectric cladding," Appl. Phys. Lett. **88**(1), 011112 (2006).
21. E. Kuramochi, H. Taniyama, T. Tanabe, A. Shinya, and M. Notomi, "Ultrahigh-*Q* two-dimensional photonic crystal slab nanocavities in very thin barriers," Appl. Phys. Lett. **93**(11), 111112 (2008).
22. M. Notomi, and H. Taniyama, "On-demand ultrahigh-*Q* cavity formation and photon pinning via dynamic waveguide tuning," Opt. Express **16**(23), 18657–18666 (2008), http://www.opticsinfobase.org/oe/abstract.cfm?URI=oe-16-23-18657.
23. E. Kuramochi, T. Tanabe, H. Taniyama, K. Kawasaki, and M. Notomi, "Ultrahigh-*Q* silicon-on-insulator one dimensional mode-gap nanocavity," in *The Conference on Lasers and Electro-Optics and The Quantum Electronics and Laser Science Conference (CLEO/QELS:2010)*, Optical Society of America, Washington, DC, USA, 2010, paper CWB2.
24. Q. Quan, P. B. Deotare, and M. Lončar, "Deterministic design of ultrahigh *Q* and small mode volume photonic crystal nanobeam cavity," in *The Conference on Lasers and Electro-Optics and The Quantum Electronics and Laser Science Conference (CLEO/QELS:2010)*, Optical Society of America, Washington, DC, USA, 2010, paper CWB5.
25. Q. Quan, P. B. Deotare, and M. Lončar, "Photonic crystal nanobeam cavity strongly coupled to the feeding waveguide," Appl. Phys. Lett. **96**(20), 203102 (2010).
26. T. Tanabe, M. Notomi, E. Kuramochi, and H. Taniyama, "Large pulse delay and small group velocity achieved using ultrahigh-Q photonic crystal nanocavities," Opt. Express **15**(12), 7826–7839 (2007), http://www.opticsinfobase.org/oe/abstract.cfm?URI=oe-15-12-7826.
27. M. Notomi, T. Tanabe, A. Shinya, E. Kuramochi, and H. Taniyama, "On-Chip All-Optical Switching and Memory by Silicon Photonic Crystal Nanocavities," Adv. Opt. Technol. (**2008**), 568936 (2008).
28. S. Mandal, and D. Erickson, "Nanoscale optofluidic sensor arrays," Opt. Express **16**(3), 1623–1631 (2008), http://www.opticsinfobase.org/abstract.cfm?URI=oe-16-3-1623.
29. C. E. Png, and S. T. Lim, "Silicon optical nanocavities for multiple sensing," J. Lightwave Technol. **26**(11), 1524–1531 (2008).

1. Introduction

One-dimensional (1D) photonic crystal (PhC) (or distributed Bragg reflector based) cavities are attractive [1–4] because of their structural simplicity and smaller size compared with higher dimension PhCs. Although two-dimensional (2D) PhC cavities have played a major role because their quality factor (Q) was developed earlier than those of 1D and three-dimensional (3D) PhC cavities, the Q values of 1D PhC cavities have been improving continuously. At first, the Q of a cavity with a 1D photonic bandgap (PBG) was less than 1000. The fine hole-position tuning [5,6] can increase the Q value to ~6×10^4 [3] and further optimization can increase it to 1.5×10^5 [4]. In these works, small modal volume (V) of less than 1 $(\lambda/n)^3$ was also crucial, which was achieved by the use of the localized mode in the 1D PBG and the sub-micron PhC width based on high silicon/air index contrast. Recently, high-Q 1D PhC cavities have been further improved by the mode-gap modulation approach, which succeeded in producing ultrahigh-Q cavities in 2D PhCs [5,7,8]. In 2008, we reported two air-bridge 1D PhC cavity designs employing the mode-gap modulation approach, namely a ladder cavity and a stack cavity, both of which showed a calculated Q of higher than 10^7 and a small V of 1.4~2 $(\lambda/n)^3$ [9]. The mode-gap approach modifies the geometry much gently in comparison with the conventional designs, which prevents decrease of Q value due to the delocalization in k-space. Despite of the gentle geometry modulation, the mode-gap approach preserves V as well as the conventional designs because the light confinement is sufficiently

#128504 - $15.00 USD Received 18 May 2010; revised 25 Jun 2010; accepted 28 Jun 2010; published 12 Jul 2010

strong in the former. In 2009, air-bridge ladder-type 1D PhC cavities with the mode-gap modulation increased the experimental Q value to $2\sim7\times10^5$ and reduced the V value to 0.4 $(\lambda/n)^3$ [10–12]. Owing to their extreme compactness, 1D PhC high-Q cavities are now suitable for realizing various devices with high performance. We have reported the ultralow power operation of thermo-optic optical switch realized by an air-bridge ladder cavity with a Q of 2.2×10^5 [12]. The air-bridge ladder cavity is also one of the best systems for opto-mechanical devices based on ultra-weak enhanced optical forces [11,13,14]. Applications to highly sensitive nano-sensors for various objects and environments [15–18] are also promising.

In this paper, we report a 1D mode-gap-based cavity in a thin silicon layer with thermal oxide (SiO_2) under-cladding, namely a silicon-on-insulator structure (SOI). Since this system is highly compatible with a silicon wire waveguide, which is a key element in silicon nanophotonics, it is important to improve the performance of the silicon-wire-based nanocavity to the level of the best 2D PhC nanocavity. Although it has been suggested that the vertical asymmetry of the SOI system might increase the coupling loss between the TE and TM modes in a 2D PhC [19,20], recent reports [3,4] strongly indicate that this loss is not serious in 1D cavities. In this work our goal is to outperform the previous record Q values (calculation: 4×10^5 [3], experiment: 1.5×10^5 [4]) by the use of the mode-gap modulation approach. In our previous paper [12] we reported an SOI 1D PhC stack mode-gap cavity with an experimental Q of 8×10^4 without detail explanation of cavity design. Here we provide a more detailed account of an SOI stack cavity with a higher experimental Q. Moreover, we report SOI ladder cavities consisting of rectangular or circular holes, where the latter achieved the highest Q value both numerically and experimentally. This design for SOI cavities also improves Q of 1D air-bridge PhC cavities both numerically and experimentally compared with our previous reports [9,12]. Another goal of this work is to realize a small V close to 0.4 $(\lambda/n)^3$ in air-bridge [10] and 0.6 $(\lambda/n)^3$ in SOI [3], because it was several times larger in our previous reports [9,12].

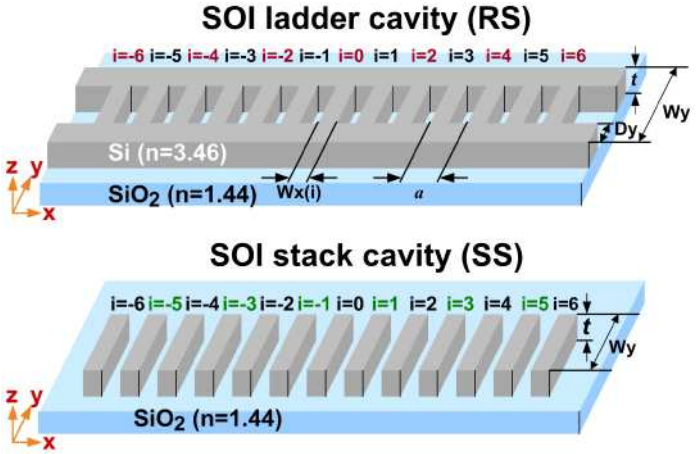

Fig. 1. 1D SOI mode-gap cavities with rectangular holes/stacks studied in this work.

#128504 - $15.00 USD Received 18 May 2010; revised 25 Jun 2010; accepted 28 Jun 2010; published 12 Jul 2010

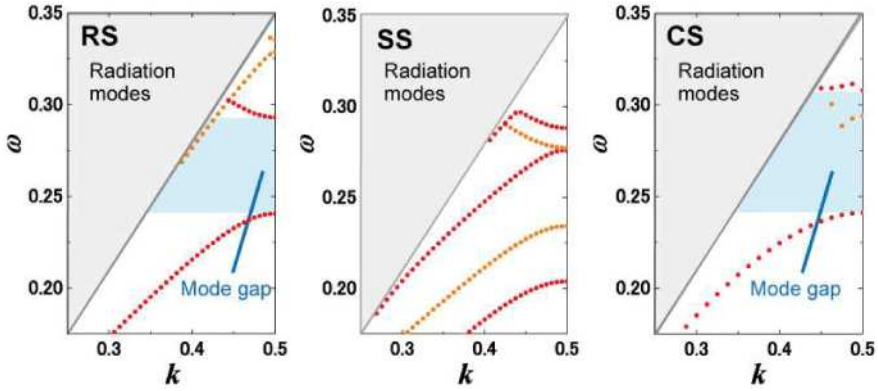

Fig. 2. Dispersion of the TE modes in the three 1D SOI PhCs obtained by 3D calculation of the R-Soft Bandsolve code. (Left:) rectangular hole ladder (RS), (Center:) rectangular stack (SS), (Right:) circular hole cavity (CS). Red dots correspond to even mode and orange dots do to odd mode. The parameters are as follows; RS/SS: $W_x(i)=0.45a$; CS: $r(i)=0.3a$, $W_y=1.35a$.

2. 1D SOI modegap cavities

Design and FDTD analysis of cavities with rectangular holes/stacks

Here we start with two types of SOI cavities, in which the air under-cladding layer of the air-bridge ladder cavity and the air-bridge stack cavity proposed in our previous paper [9] (and shown in Fig. 7 where they are denoted by RA and SA, respectively) is simply replaced with an SiO_2 layer as shown in Fig. 1. As we describe below, the lowest band (dielectric band) is used throughout our work for the cavity mode. This is because we believe that the use of the band farthest from the light cone might make the cavity durable as regards the loss related to the light cone. This could be advantageous because the impact of the light cone is much more serious in an SOI cavity than in an air-bridge cavity. We employed a parabolic modulation function that achieved a very high Q (~10^8) in the air-bridge cavities [9]: $W_x(i)=W_{x0}(1+(i/m)^2)$ ($W_{x0}=0.45a$, $m=28$); otherwise $W_x(i)=W_x(i_{max})$ when $i> i_{max}$ ($i_{max}=14$). The size of the air hole (the air gap in the stack cavity) is maximum at the cavity center and decreases monotopically as it is away from the center. An parameter set of an SOI ladder cavity (denoted by RS in Fig. 1) is as follows; lattice constant a, silicon ($n=3.46$) layer thickness $t=0.5a$, PhC Width $W_y=1.75a$, and side beam width $D_y=0.25a$. The width of the ladder rungs $W_x(i)$ (or x length of the stack i), which is a function of the position i numbered from the center of the cavity, is modulated to introduce a mode-gap confined mode. An example parameter set of the SOI stack cavity (denoted by SS in Fig. 1) is as follows; $t=0.5a$, $W_y=4a$, and $W_x(i)=W_{x0}(1+(i/m)^2)$ ($W_{x0}=0.45a$, $m=28$, $i_{max}=14$)) [9].

The dispersion of the waveguide modes of the 1D PhC corresponding to the SOI cavities (RS/SS) is shown in Fig. 2. The dispersion curves are basically similar to that of the 1D air-bridge PhC [9], thus allowing the use of the same mode-gap modulation approach. The lowest band used for the cavity mode is remotely located under the light line at the mode edge (K point) even with the SiO_2 cladding, which would be advantageous in obtaining high Q. This is because the mode edge (at the K point) is very far from the light cone, which might suppress the impact of the high order lossy mode adjacent to light cone. Moreover, we believe that the large interval between the fundamental and higher order modes at the mode edge would allow the existence of an ultrahigh-Q mode in the stack cavity (SS) despite the lack of a mode-gap as shown in Fig. 2.

Here we focus only on the fundamental resonant mode although the cavities studied here have several high order modes. The same full 3D FDTD code used in previous reports [8,21,22] was used to analyze these cavities numerically. Figure 3 shows mode profiles of the

#128504 - $15.00 USD Received 18 May 2010; revised 25 Jun 2010; accepted 28 Jun 2010; published 12 Jul 2010

two SOI cavities whose parameters are shown in the caption. The Q value, resonant

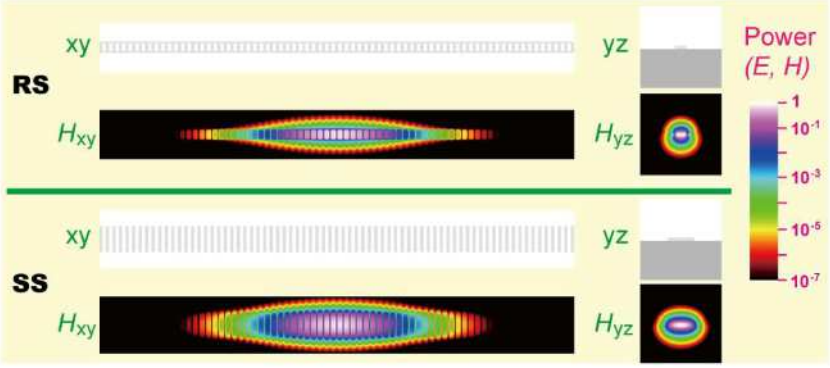

Fig. 3. Electromagnetic mode distribution profiles of the fundamental resonant mode of the rectangular hole/stack (RS/SS) cavities obtained by 3D FDTD calculation. Lattice constant a=420 nm, for both cavities. xy (H_{xy}) means the distribution in the xy plane. H indicates the power (sum of square of field component for all directions) of the magnetic field.

wavelength λ_c, and V of the fundamental mode of the SOI ladder cavity (RS) were found to be 2.7×10^7, 1720 nm, and 1.5 $(\lambda/n)^3$, respectively. For the SOI stack cavity (SS), the Q, λ_c, and V of the fundamental mode shown in Fig. 3 were 1.8×10^7, 1798 nm, and 2.0 $(\lambda/n)^3$, respectively. These Q values are two order of magnitude higher than those of the 1D SOI cavities previously reported [3,4] and now they are comparable with those of the ultrahigh-Q 2D PhC cavities [7,8,21]. The result also suggests that the vertical asymmetry of the SOI structure does not seriously affect the Q value. Notice that although the SOI cavities require a wider W_y than the air-bridge cavities (1.5a for the ladder cavity (RA) and 3a for the stack cavity (SA)), the mode volume for RS and SS cavities is comparable to that for corresponding air-bridge cavities (RA ans SA).

Design and FDTD analysis of cavities with circular holes

Although we only considered rectangular holes in our previous paper [9], here we add a 1D mode-gap cavity consisting of circular holes. A circular shape is the most widely used hole shape for 2D/1D PhCs and we have developed a technique for the high precision nano-fabrication of a 2D PhC slab with circular holes that has realized a cavity with an experimental Q value of over 10^6 [21]. Therefore, a design that allows a 1D circular hole cavity to have an ultrahigh-Q value must be important. Here we study a 1D SOI ladder cavity with circular holes (CS), as shown in Fig. 4, where the radius r(i) is given as a parabolic function: $r(i)=r_0(1-(i/m)^2)$ (r_0=0.3a) as long as r(i) is larger than a given minimum value r_{min}. Very recently, we [23] and Q. Quan et al. [24,25] independently found that this design realized an ultrahigh Q value in air-bridge cavities. Figure 4 also shows the mode profiles of the cavity (CS) for a, W_y, and m values of 400 nm, 540 nm, and 21, respectively. The Q, λ_c, and V of the mode were 2.9×10^8, 1660 nm, and 0.78 $(\lambda/n)^3$, respectively. We found that the circular hole cavity can have a higher Q and a smaller V than the corresponding rectangular hole cavity (RS). Figure 5 shows the calculated Q, λ_c, and V values of the cavity (CS). These data exhibit a clear dependence on the specific structural parameter. Q was always higher than 10^7 at m>=21 and W_y>=500 nm. Q was even higher than 10^8 when W_y was between 540 and 620 nm. When m was reduced from 20, Q dropped rapidly. A W_y of 400 nm or narrower also reduced Q significantly. Thus, it seems that a W_y of around 600 nm (W_y /a~1.5) is the best for the SOI cavity (CS) to realize the highest Q. The relation between λ_c and V is also interesting. λ_c changed greatly as W_y varied. The wide tunability range of λ_c (at least 200 nm), while maintaining a very high Q, obtained by changing W_y might be useful in certain device applications. The dependence of λ_c on m is relatively small. In contrast, V depended strongly on m and slightly on W_y. The change is almost linear with m. It is important to note that when

#128504 - $15.00 USD Received 18 May 2010; revised 25 Jun 2010; accepted 28 Jun 2010; published 12 Jul 2010

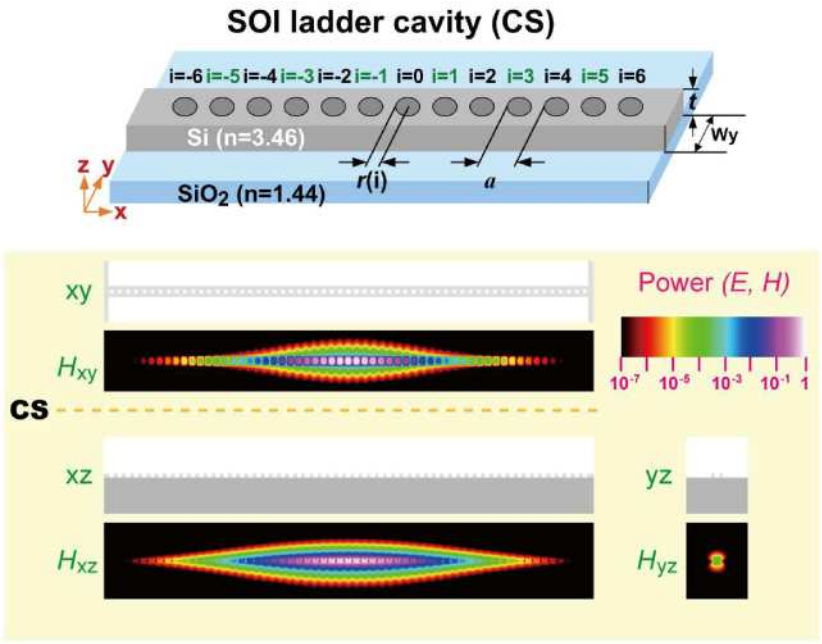

Fig. 4. The design and calculated electromagnetic mode distribution profiles (fundamental resonant mode) of the SOI circular hole ladder cavity (CS). The parameters are as follows; a=400 nm, m=21, r_{min}=0.22a, W_y=1.35a; RS: a=420 nm, SS: a=420 nm.

W_y >500 nm, V was nearly unchanged with changes in W_y despite the significant change in λ_c. V can be minimized by maximizing m although too small an m causes a considerable reduction in Q.

When we compare a circular hole cavity (CS) with a rectangular hole cavity (RS) we find two major differences. (1) The former exhibited a higher Q for a wide range of W_y (although the latter showed a sufficiently high Q), and (2) V was 0.5~1 $(\lambda/n)^3$ in the former and 1.4~2.1 $(\lambda/n)^3$ in the latter. Although we have not yet determined the mechanism explaining why circular holes are better than rectangular ones, a detailed analysis of the FDTD data suggested that both the electric and magnetic field mode profiles for RS/RA exhibit singular distribution around the rectangular corners, which were not found in CS/CA. We speculate that the difference originates from this feature. Moreover, when we replaced every hole (i) of the circular hole cavity (CS) with a square hole with a side length of 1.8r(i) (this replacement roughly maintained the filling factor) Q fell to around 10^6 and V was larger than 1 $(\lambda/n)^3$. Thus, our data demonstrated that numerically the circular hole cavity performed better than the rectangular hole cavity.

Experimental results

We fabricated Si PhC cavities in the thin (~210 nm) SOI layer of commercial SOI wafers that have a thick (3 μm) SiO_2 layer (BOX). We used a previously reported fabrication process [8,21,23]. The PhC pattern was drawn in a positive electron beam resist film coated on the wafer with a 100 kV electron beam writer. Then the SOI layer was patterned with an inductively coupled plasma etcher using an SF_6/C_4F_8 gas mixture. The resist film was then removed and the wafer was cleaned. Since the characteristics of the cavities were evaluated using a transmission measurement via input/output wavguides coupled with cavities, the thickness of the 1D barrier between cavities and waveguides, namely the number of holes/stacks, was changed to control the horizontal component of Q (Q_H). When we define i

#128504 - $15.00 USD Received 18 May 2010; revised 25 Jun 2010; accepted 28 Jun 2010; published 12 Jul 2010

of the element (rung/stack/circular hole) at the edge of the barrier as N_{max}, it was between 14

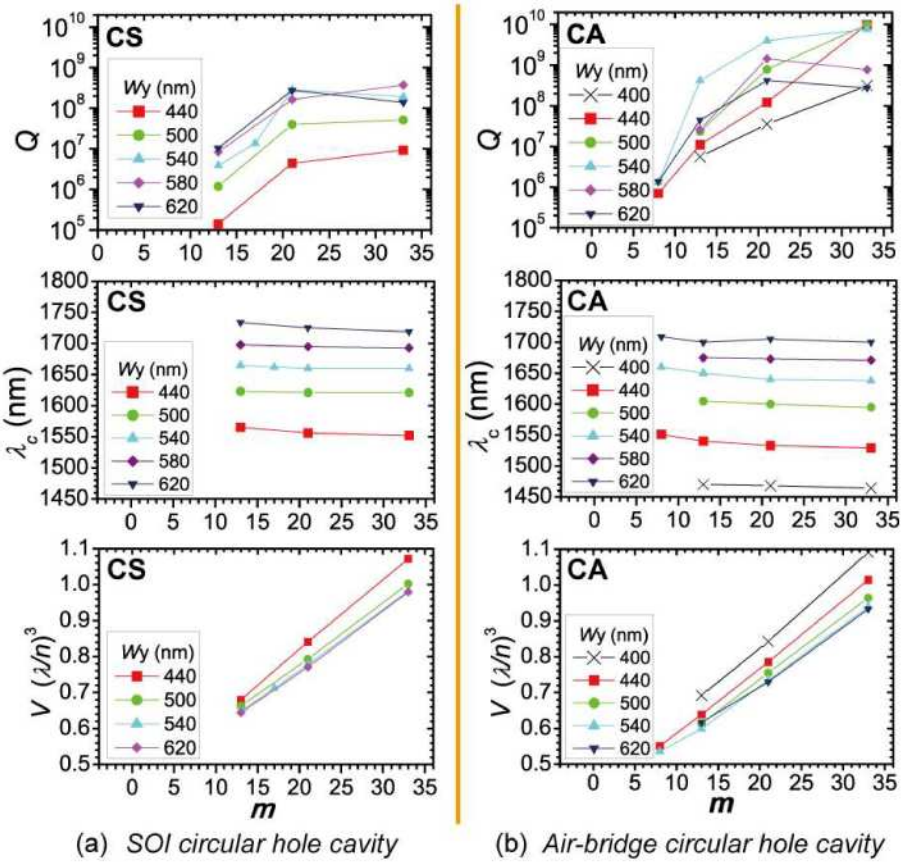

Fig. 5. Q, λ_c, and V of the fundamental resonant mode of the circular hole cavities as a function of m calculated by the FDTD (a=400 nm, r_{min}=0.22a). (a) SOI cavity (CS); (b) air-bridge cavity (CA).

and 21 in this study. In the rectangular hole cavity (RS) there was no air hole between the edge ladder rung and the external waveguide part. Total number of holes was $2\times N_{max}+1$. In experiment, a of the rectangular hole cavity (RS) and stack cavity (SS) was reduced down to 378 and 362 nm, respectively from 420 nm assumed in calculation, where all other parameters except for the SOI layer thickness (constant at 210 nm) were scaled down with a. This reduction was designed to shift λ_c in the range of our measurement system (the long wavelength limit was 1630 nm). Even after the great modification of the geometry, numerical data except λ_c was preserved (Q, λ_c, and V were 3.3×10^7, 1586 nm, and 1.4 $(\lambda/n)^3$ for RS and 1.8×10^7, 1597 nm, and 1.9 $(\lambda/n)^3$ for SS, respectively), which demonstrated again that the 1D ultrahigh-Q and small-V mode was robust for structural modification and thereby held wide tunablility of λ_c as demonstrated in the cavities with circular holes (Fig. 5). In the circular hole cavities (CS), a was 400 nm both in calculation and in experiment. Figure 6(a) shows scanning electron microscope (SEM) images of fabricated cavity samples. The following are the parameters of the fabricated samples measured with a SEM. For the rectangular hole cavity (RS), W_{x0}, W_y, and D_y were ~190, 675, and 100 nm, respectively. For the rectangular stack cavity (SS), W_y was 1450 nm and W_{x0} was 175 nm. For the circular hole cavity (CS), r_0 was 130 nm and m (21,33) and W_y (450, 490, 530 nm) were modified.

We used the same measurement set-up that we employed for the measurements of ultrahigh-Q 2D PhC nanocavities [21,26]. We focused on the TE (TE-like) mode and we

#128504 - $15.00 USD Received 18 May 2010; revised 25 Jun 2010; accepted 28 Jun 2010; published 12 Jul 2010

chose the mode using a polarizer and a polarization maintained fiber. A pair of lensed fibers

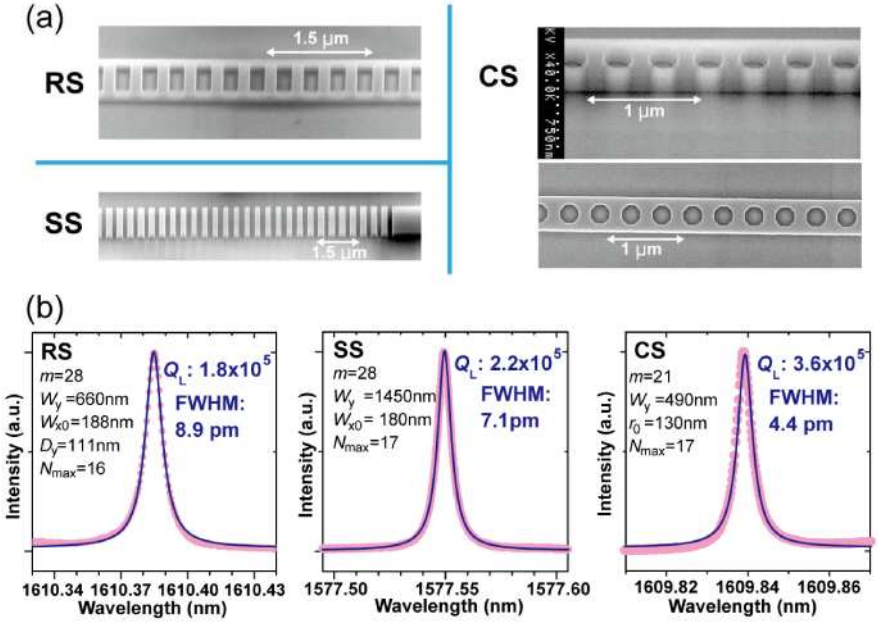

Fig. 6. (a) SEM images of the fabricated 1D SOI cavity samples. (b) Transmission spectrum of the fundamental resonant mode of the 1D SOI cavity samples. Linewidth (full width at half maximum: FWHM) was determined by Lorentz fitting (blue line). The lower right graph shows the Q_L dependence on the cavity width W_y .

was used to maximize the coupling to the waveguides on the sample. The experimental Q (loaded Q, Q_L) of the cavity mode was determined from the transmission spectrum. The unloaded Q (Q_{UL}) expressed as $Q_{UL}=1/(Q_L^{-1}- Q_H^{-1})$ is usually smaller than the calculated Q because of excess radiation loss mainly caused by fabrication errors and absorption loss. The experimental Q was evaluated by using the linewidth and λ_c of the cavity mode. The spectra accompanied Fabry-Perot oscillations of several dB due to the facets at the edge of the sample. However, the impact of the oscillations on the determination of Q_L by Lorentz fitting was negligible because the resonant mode (linewidth was 10 pm or less: here we focused on high- Q_L/high-Q_H samples) was completely distinguishable from the oscillations (it was over 20 pm) and the peak to background level ratio of the resonant mode was higher than 10. The input power was minimized as the carrier absorption loss and thermo-optic effect could be ignored.

Figure 6(b) shows transmission spectra corresponding to the best Q_L value for every type of cavity. The accurate control of Q_H by adjusting N_{max} was difficult in this study and Q_H fluctuated considerably for a specific N_{max} value. As N_{max} was increased from 14 (15) to 17 (18), the average transmittance value (averaged among many equivalent samples) normalized to the reference silicon wire waveguide decreased nearly linearly from −5 to −20 dB in the stack cavity (the rectangular hole cavity) but the error bar was 10 dB. In the circular hole cavity, the average transmittance varied more gradually (−5 dB at N_{max}=14 and −20 dB at N_{max}=18) but the error bar was also large (10 dB). Although we do not know exact origin of the error bar (it was partly affected by the Fabry-Perot oscillations), we believe that coupling between the 1D cavities studied here and the external waveguide is highly sensitive to fabrication errors in 1D PhC. The optimum N_{max} values for Q_L values of ~2×10^5 and ~6×10^5 were 15-18 and 17-20, respectively. Note that the relation between N_{max} and transmittance depends on the strength of geometry modulation m.

We found that in all the rectangular hole/stack cavities, Q_L was limited to around 2×10^5. The best Q_L values were 1.8×10^5 and 2.2×10^5 for the ladder cavity (RS) and the stack cavity

#128504 - $15.00 USD Received 18 May 2010; revised 25 Jun 2010; accepted 28 Jun 2010; published 12 Jul 2010

(SS), respectively. The latter value was improved against our previous report [9,12], and the

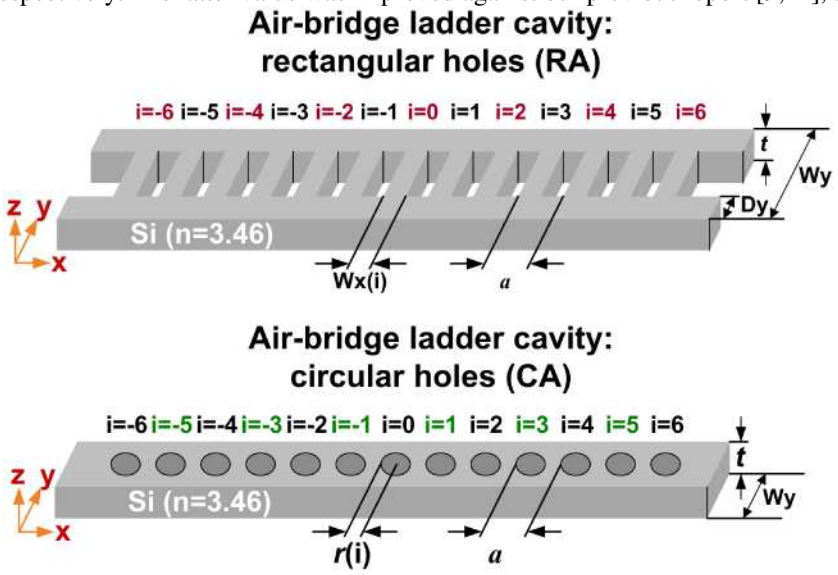

Fig. 7. 1D Si air-bridge mode-gap cavities studied in this work.

best data for 1D stack cavities. By contrast, the circular hole ladder cavity (CS) exhibited a much better Q_L despite the fact that the same SOI wafer and the fabrication technology were used. The best Q_L values for CS were 3.6×10^5 (m=21) and 3.1×10^5 (m=33) for a W_y of 490 nm. respectively. The former was not only record data for an SOI PhC cavity but also the best Q/V value of those (corresponding V was ~0.78 $(\lambda/n)^3$). Although we have a sample with a W_y value of 530 nm, its λ_c was beyond the range of the measurement system.

3. 1D air-bridge modegap cavities

Design and FDTD analysis

Since the design and performance of the rectangular hole ladder cavity have already been reported [9], here we report only the design of the circular hole ladder cavity that is added because it demonstrated superior Q over the rectangular hole in the case of SOI cavity. The design shown in Fig. 7 and denoted by CA is the same as that of the SOI cavity (CS) except for the under-cladding material. The radius r(i) is also given as $r(i)=r_0(1-(i/m)^2)$ (r_0=0.3a). Figure 6(b) shows the calculated Q, λ_c, and V values of the air-bridge circular hole cavity (CA). The results are qualitatively similar to those of the SOI cavity (CS) shown in Fig. 6(a) but the optimum W_y for high Q was ~540 nm (W_y /a~1.5) which was ~600nm in the SOI cavity. The circular hole cavity (CA) exhibited a Q value about one order of magnitude higher than that of the SOI cavity (CS) and the air-bridge rectangular hole cavity (RA, 10^7~10^8) [9]. The relationship between λ_c and V shown in Fig. 6(b) was also almost the same as with the SOI cavity shown in Fig. 6(a), although λ_c was blue-shifted in the air-bridge cavity. Regardless of this, the λ_c of the cladding material was highly sensitive to the ladder width W_y, and V was controlled by the strength of the modulation m in these 1D cavities. V was also in the 0.5~1 $(\lambda/n)^3$ range in the air-bridge circular hole cavity (CA), which is difficult to achieve with the air-bridge rectangular hole cavity (RA) and the air-bridge rectangular stack cavity (SA) [9].

Experimental results

The air-bridge cavities were prepared and measured in the way described in section 2.3. To realize the air-bridge structure, the BOX layer around the PhC was removed by dipping it in

#128504 - $15.00 USD Received 18 May 2010; revised 25 Jun 2010; accepted 28 Jun 2010; published 12 Jul 2010

buffered HF after the dry etching of the SOI layer. The a value of the rectangular hole cavity

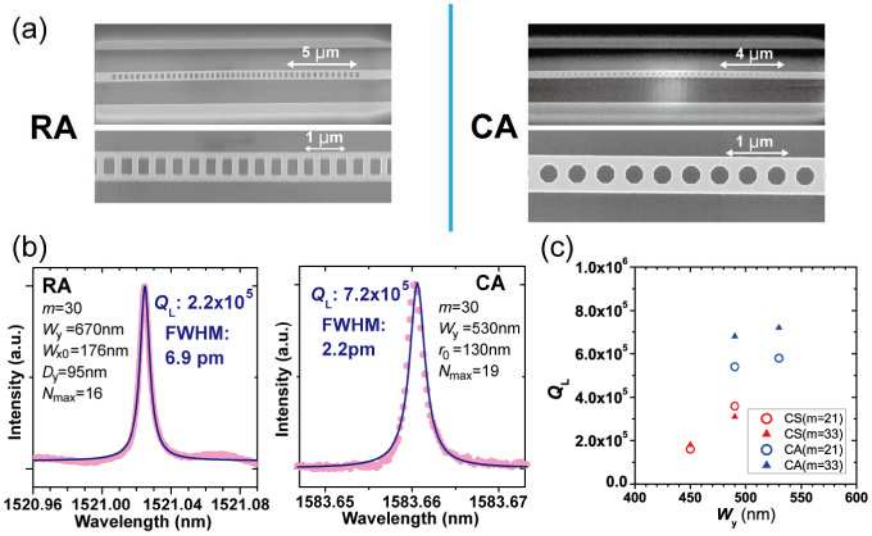

Fig. 8. (a) SEM images of the fabricated Si air-bridge ladder cavity samples. (b) Transmission spectrum of the fundamental resonant mode of the air-bridge ladder cavity samples. (c) Plot of the experimental Q of the circular hole ladder cavities (CS: SOI, CA: air-bridge) as a function of the cavity width W_y.

(RA) and the circular hole cavity (CA) were 386 nm and 400 nm, respectively. After rescaling of a (386 nm) the calculated Q, λ_c, and V for RA were 2.4×10^8, 1581 nm, and 1.4 $(\lambda/n)^3$, respectively. Figure 8(a) shows SEM images of fabricated cavity samples. The hole size and radius of these samples were the same as those of the corresponding SOI cavities described in Section 2.3. Both λ_c and m were changed as with the SOI cavities.

Figure 8(b) shows transmission spectra corresponding to the best Q_L value of every type of cavity. The best Q_L (2.2×10^5) of the air-bridge cavity (RA) is the same as the previously reported value [12]. By contrast, the best Q_L of the air-bridge cavity (CA) was also increased to 7.2×10^5, which is nearly three times higher than the rectangular hole cavity and almost with the same as the data reported by P. B. Deotare et al. [10].

Figure 8(c) summarizes the experimental Q values obtained in this study for all types of cavity. The results suggest that the experimental Q value depends on the cavity width W_y. Another important suggestion is that the Q of the cavities consisting of rectangular shaped elements (RS, RA, and SS) was restricted to around 2×10^5 regardless of the cladding material whereas the Q values of the circular hole cavities (CS and CA) were clearly not limited to 2.2×10^5. Therefore, although the latter has a better numerical Q than the former, it appears that the restriction in experiment was due to some experimental problem such as fabrication error. It suggests that the circular hole ladder cavities may be relatively robust in terms of problems related to fabrication.

4. Summary

We have reported detailed numerical characteristics of ultrahigh-Q 1D SOI mode-gap nanocavities with corresponding air-bridge nanocavities that we studied using 3D FDTD analysis. By employing circular holes, we reduced V to less than 1 $(\lambda/n)^3$ while maintaining Q in the of 10^7-10^9 range, which is difficult to accomplish with a design using rectangular shaped elements. The advantage of the SOI circular hole cavity was clearly demonstrated in an experiment where it achieved a Q as high as 3.6×10^5, whereas in cavities with rectangular holes/stacks, Q was limited to around 2×10^5. The circular hole ladder cavity is unique not only for its ultrahigh Q and ultrasmall V but also for the wide range tunability of λ_c that can be realized by changing the lateral width W_y. A 1D SOI PhC cavity system has no disadvantage

#128504 - $15.00 USD Received 18 May 2010; revised 25 Jun 2010; accepted 28 Jun 2010; published 12 Jul 2010

in comparison with 2D air-bridge PhC cavities as regards numerical performance, and so the former is a strong alternative to the latter although in practice the radiation loss and Q_H fluctuation should be further reduced. The great advantage of the SOI circular hole cavity (CS) is clearly its very high compatibility with Si nanophotonics, whereas a wider waveguide width is needed for the rectangular hole/stack cavities (RS and SS). In terms of the air-bridge cavity, the performance is similar to that of the SOI cavity but an up to 10 times higher Q is expected. The meaning of achieving a Q value of 7.2×10^5 in a circular hole cavity (CA) is not simply that it reproduces the result reported by Deotare et al. [10]. It also shows that the Q value is ready for integrated photonics applications [27] since our data are achieved in a waveguide-cavity coupled system. Moreover, we revealed that the problem of the rectangular elements is also crucial for 1D air-bridge cavities. Therefore, we believe that this finding will be of considerable help in relation to the design of the various 1D cavities including cavities for opto-mechanics [11,13,14], photonics devices [12], and sensors [28,29].

Acknowledgments

We thank Dr. Atsushi Yokoo, Dr. Akihiko Shinya, and Dr. Hisashi Sumikura for fruitful discussions. We thank Daisuke Takagi, Junichi Asaoka, and Dr. Toshiaki Tamamura for fabricating the samples.

#128504 - $15.00 USD Received 18 May 2010; revised 25 Jun 2010; accepted 28 Jun 2010; published 12 Jul 2010